Available online at www.sciencedirect.com
SCIENCE DIRECT®
International Journal of Heat and Mass Transfer 47 (2004) 5045–5057
International Journal of HEAT and MASS TRANSFER
www.elsevier.com/locate/ijhmt

Nucleate pool-boiling heat transfer. II: assessment of prediction methods

I.L. Pioro [a,*], W. Rohsenow [b], S.S. Doerffer [c]

[a] Chalk River Laboratories, AECL, Chalk River, Ont., Canada K0J 1J0
[b] Mechanical Engineering Department, Massachusetts Institute of Technology, Cambridge, MA 02139-4307, USA
[c] AECL, Sheridan Park, Mississauga, ON, Canada L5K 1B2

Received 19 August 2003; received in revised form 22 June 2004
Available online 23 August 2004

Abstract

Part I of this paper has identified all significant boiling surface parameters affecting nucleate pool-boiling heat transfer and has investigated their parametric trends, thus providing a measure of the state of the art in this area. This part of the paper examines the existing prediction methods for the heat transfer coefficient (HTC) under this boiling regime. Six heat transfer pool-boiling correlations that are well known in the literature have been selected and their prediction accuracy has been assessed against available and well-documented experimental databases. These databases provide HTCs obtained: (i) under pool-boiling conditions of fluids such as water, ethanol, R-113, and *n*-heptane; and (ii) on the following large-size horizontal surfaces: thick plates (made of copper, aluminum, brass, and stainless steel), and a horizontal circular disk (plated with a thin layer of polished chromium). For completeness, the microgeometry characteristics of several boiling surfaces are included here, even though they are not fully utilized in the present analysis. The surface microgeometry has been characterized by 14 roughness parameters measured with a laser profilometer.

The analysis concludes that within the investigated ranges of boiling conditions, working fluids and boiling surfaces, the Rohsenow and Pioro nucleate pool-boiling correlations are the most accurate among those assessed. The Rohsenow and Pioro correlations use constants and powers for non-dimensional numbers that correspond to a specific surface–fluid combination, as opposed to the other correlations that use fixed values regardless of the surface–fluid combination.

1. Introduction

In general, the nucleate pool-boiling heat transfer coefficient (HTC) is proportional to the heat flux or a non-dimensional number containing the heat flux term (for example, the Kutateladze number (K)) raised to the power of about 2/3. The effect of thermophysical properties, including the indirect effect of saturation pressure, is usually expressed through the Prandtl number (Pr) raised to some power.

There are two typical approaches used to determine the HTC for the boiling process under consideration:

* Corresponding author. Tel.: +1 613 584 8811x4805; fax: +1 613 584 8213.
E-mail address: pioroi@aecl.ca (I.L. Pioro).

0017-9310/$ - see front matter © 2004 Elsevier Ltd. All rights reserved.
doi:10.1016/j.ijheatmasstransfer.2004.06.020

Nomenclature

c	specific heat [$J\,kg^{-1}\,K^{-1}$]
C_{sf}	coefficient in the Rohsenow correlation (see Eq. (1))
C^*_{sf}	coefficient in the Pioro correlation (see Eq. (2))
D	diameter [m]
D_b	vapor bubble departure diameter [m]
f	frequency of vapor bubble departure [s^{-1}]
g	acceleration due to gravity [$m\,s^{-2}$]
h	heat transfer coefficient [$W\,m^{-2}\,K^{-1}$]
H_{b-c}	distance between boiling and condensing surfaces [mm]
h_{fg}	latent heat of vaporization [$J\,kg^{-1}$]
H_{WF}	working-fluid level [mm]
k	thermal conductivity [$W\,m^{-1}\,K^{-1}$]
l_*	pool-boiling characteristic dimension, $\left[\frac{\sigma}{g(\rho-\rho_g)}\right]^{0.5}$ [m]
p	pressure [Pa]
R_a	arithmetic-average roughness [μm]
R_q	root-mean-square roughness [μm]
q	heat flux [$W\,m^{-2}$]
T	temperature [°C]

Greek symbols

α	thermal diffusivity, $\left[\frac{k}{c_p\rho}\right]$ [$m^2\,s^{-1}$]
Δ	difference
δ	wall thickness [m]
μ	dynamic viscosity [Pa s]
θ	contact (wetting) angle [degrees]
ρ	density [$kg\,m^{-3}$]
σ	surface tension [$N\,m^{-1}$]
v	kinematic viscosity $\left[\frac{\mu}{\rho}\right]$ [$m^2\,s^{-1}$]
χ	thermal assimilability of solid $\sqrt{kc\rho}$ [$J\,m^{-2}\,K^{-1}\,s^{-0.5}$]

Greek symbols

b	boiling
c	condensation
cr	critical
exp	experimental
f	saturated fluid
g	saturated vapor
p	at constant pressure
pred	predicted
s	saturation
sf	surface–fluid
WF	working fluid
Note:	physical properties with no subscript refer to saturated liquid

Non-dimensional numbers

K	Kutateladze number, $\frac{q}{h_{fg}\sqrt{\rho_g}[g\sigma(\rho-\rho_g)]^{0.25}}$
Nu_b	nucleate-pool-boiling Nusselt number, $\frac{h_b l_*}{k}$
Pr	Prandtl number, $\frac{c_p\mu}{k}$

Abbreviations

HTC	heat transfer coefficient
rms	root-mean-square
St. St.	stainless steel

- The first approach is characterized by using constant values for the coefficients and powers; this applies to a large variety of fluids and boiling conditions (the correlations of Kutateladze [1,2], Labuntsov [3], Kruzhilin [4], and others). The main advantage of this approach is the wide range of applicability of these correlations, regardless of the kind of fluid and boiling surface; however, the prediction accuracy of this approach may be sacrificed.
- The second approach is based on the variability of: (i) the coefficients in a correlation according to the surface–fluid combination (the Rohsenow original correlation [5]—coefficient C_{sf}), or (ii) the power values (usually for the Prandtl number), depending on the fluid type. The modified Rohsenow correlation [6] employs the variable coefficient C_{sf}, and the Prandtl number is raised to a constant power; that is, one value for water, and another value for the remaining fluids (the term "fluids" does not usually include cryogenic liquids and liquid metals). The latest analysis conducted by Pioro [7] showed that higher prediction accuracy of the Rohsenow correlation could be achieved by varying the power in the Prandtl number according to the surface–fluid combination. The main advantage of this approach, when the correlation is used for the investigated surface–fluid combinations, is higher prediction accuracy than that obtained from the correlations corresponding to the first approach. However, a disadvantage of the second approach is the limitation for application of the correlation outside the investigated surface–fluid combinations. Even though the second approach provides better prediction accuracy of the boiling HTC, the effects of boiling surface properties and characteristics, and interactions between the solid, liquid and vapor components are still not properly

Table 1
Nucleate pool-boiling heat-transfer correlations

Author	Correlation	
Rohsenow [5,6]	$\frac{c_p\Delta T_b}{h_{fg}} = C_{sf}\left[\frac{q}{\mu h_{fg}}\sqrt{\frac{\sigma}{g(\rho-\rho_g)}}\right]^{0.33}\left(\frac{c_p\mu}{k}\right)^n$ and $h_b = \frac{q}{\Delta T_b}$, where C_{sf} is the constant, depended upon the nature of the heating, surface–fluid combination and n is the power (for values of C_{sf} and n see [7]).	(1)
Pioro [11]	$Nu = C^*_{sf}K^{\frac{2}{3}}Pr^m$ or $\frac{h_b l_*}{k} = C^*_{sf}\left\{\frac{q}{h_{fg}\rho_g^{0.5}[\sigma g(\rho-\rho_g)]^{0.25}}\right\}^{\frac{2}{3}}Pr^m$ where C^*_{sf} is the constant, depended upon the nature of the heating surface–fluid combination and m is the power (for values of C^*_{sf} and m see [11]).	(2)
Kutateladze (“new”) [2]	$Nu_* = 3.37\times10^{-9}K^{-2}M_*^{-4}$ where $Nu_* = \frac{h_b l_*}{k}$, $K = \frac{h_{fg}h_b}{c_p q}$, $M_*^4 = \frac{\frac{\sigma g}{\rho-\rho_g}}{\left(\frac{p}{\rho_g}\right)^2}$ and $h_b = \left[3.37\times10^{-9}\frac{k}{l_*}\left(\frac{h_{fg}}{c_p q}\right)^{-2}M_*^{-4}\right]^{\frac{1}{3}}$.	(3)
Kutateladze (“old”) [1]	$Nu = 0.44K_*^{0.7}Pr^{0.35}$ or $\frac{h_b l_*}{k} = 0.44\left(\frac{1\times10^{-4}qp}{gh_{fg}\rho_g\mu}\frac{\rho}{\rho-\rho_g}\right)^{0.7}Pr^{0.35}$	(4)
Labuntsov [3]	$h_b = 0.075\left[1+10\left(\frac{\rho_g}{\rho-\rho_g}\right)^{0.67}\right]\left(\frac{k^2}{\upsilon\sigma(T_s+273.15)}\right)^{0.33}q^{0.67}$	(5)
Kruzhilin [4]	$\frac{h_b l_*}{k} = 0.082\left(\frac{h_{fg}q}{g(T_s+273.15)k}\frac{\rho_g}{\rho-\rho_g}\right)^{0.7}\left(\frac{(T_s+273.15)c_p\sigma\rho}{h_{fg}^2\rho_g^2 l_*}\right)^{0.33}Pr^{-0.45}$	(6)

identified (these effects are only accounted for indirectly through the variable values of the constant and exponential power for the Prandtl number).

For the above reasons, the existing prediction methods for calculating the nucleate pool-boiling HTC should be reviewed and examined. The following section of this paper provides the assessment of six heat transfer pool-boiling correlations.

2. Assessment of pool-boiling correlations

2.1. Basis for analysis

To achieve the objective of this paper it was decided to select six well-known nucleate pool-boiling correlations and compare their prediction accuracy against the reliable experimental databases. The databases have to cover a wide range of boiling conditions, including various combinations of different fluids and boiling surfaces.

Two experimental sets of nucleate pool-boiling data [8–11] were chosen to serve as the basis for comparison of the selected heat transfer correlations. The first database covers nucleate pool boiling of the following fluids: water, ethanol, and R-113. These experiments were performed on horizontal large-size thick metal plates (without special surface treatment) made of copper, aluminum, brass, and stainless steel (surface-roughness parameters are listed in Table A1.1 of Appendix A).

The second database contains the well-known experimental data of Cichelly and Bonilla [8] for water, ethanol, and *n*-heptane boiling on a thick horizontal copper disk plated with a thin layer of polished chromium. However, these experimental data do not contain a full set of surface-roughness parameters of the boiling surface. Also, the boiling surface is a compound one. In this case, the surface–fluid combination is fluid-polished chromium; however, the conjugated heat transfer (i.e., heat transfer inside the plate linked with that at the boiling surface) can be affected by the thermophysical properties of copper.

2.2. Prediction accuracy of nucleate pool-boiling correlations

For the purpose of this analysis, six nucleate pool-boiling HTC correlations have been selected, which were developed by Kruzhilin [4], Kutateladze (the so-called “new” correlation) [2], Kutateladze (the so-called “old” correlation) [1], Labuntsov [3], Pioro [11] and Rohsenow [5] [1].

[1] C_{sf} values for the surface–fluid combinations used in the current comparison were not listed in [5]. Therefore, they were taken from [7].

Table 2
Investigated ranges and accuracy of correlations

Fluid–surface	C_{sf}	n	$C^*_{sf} \times 10^{-3}$	m	T_s, °C	ΔT_b, °C	q, kW m^{-2}	h_b, kW m^{-2} K^{-1}	Correlation	Mean error, %	RMS error, %
1	2	3	4	5	6	7	8	9	10	11	12
Water/ copper$_{\text{plate oxidized, } Ra = 1.37}$	0.017	0.76	1.228	−1.1	23–82	5.2–11.9	1.8–72	0.26–6.1	Rohsenow	0.95	14
									Pioro	4.4	14.7
									Kruzhilin	−3.8	14.9
									Labuntsov	−18.9	22.4
									Kutateladze (old)	−26.8	28.3
									Kutateladze (new)	44.4	50.6
Water/ aluminum$_{\text{plate oxidized, } Ra = 3.61}$	0.011	1.26	1.65	−1.6	3.6–102	5.2–22.4	1.3–90	0.09–9.7	Rohsenow	2.5	14.9
									Pioro	2.5	14.9
									Kutateladze (old)	−3.7	24.5
									Kruzhilin	35.5	53.5
									Labuntsov	25.3	57.1
									Kutateladze (new)	124.1	160.2
Water/brass$_{\text{plate, } Ra = 0.47}$	0.015	0.81	1.434	−1.2	14–103	3.7–15.4	1.2–144	0.18–10.6	Rohsenow	0.3	14.4
									Pioro	0.3	14.4
									Kruzhilin	−9.5	17.4
									Labuntsov	−23.4	27.3
									Kutateladze (old)	−32	33.5
									Kutateladze (new)	35.1	50.7
Water/ chromium$_{\text{polished thin layer on circular copper plate}}$ [8]	0.019	0.45	1.465	−1.2	100–205	8.3–17.7	140–656	14.6–51	Rohsenow	−1.1	7.8
									Pioro	1.5	8.5
									Kutateladze (new)	6.8	14.4
									Kutateladze (old)	−8.4	21
									Labuntsov	−21.3	21
									Kruzhilin	9.3	23.4
Water/ St. St.$_{\text{plate, } Ra = 0.75}$	0.015	0.69	1.503	−1.1	30–103	4–13.2	5–40	1–6.2	Rohsenow	3	21
									Pioro	3	21
									Kruzhilin	−20.1	27.1
									Kutateladze (new)	13.4	28.5
									Labuntsov	−33.2	37.2
									Kutateladze (old)	−40.6	46.6

Ethanol/ aluminum$_{plate}$ oxidized, $Ra = 3.61$	0.0081	1.18	51.964	−2.23	16–78	11–21.1	2.7–32	0.16–2.3	Rohsenow	1.9	4.8
									Pioro	2.3	4.9
									Kruzhilin	1.7	10.2
									Labuntsov	−3.8	13.6
									Kutateladze (old)	−27.6	27.9
									Kutateladze (new)	109.8	114.2
Ethanol/brass$_{plate}$, $Ra = 0.47$	0.0107	0.93	38.536	−1.97	30–80	5.9–14.7	2.2–56	0.37–4.7	Rohsenow	1.7	17.1
									Pioro	2.5	17.1
									Kruzhilin	−27.4	29.9
									Labuntsov	−32.5	38.9
									Kutateladze (old)	−46.9	47.7
									Kutateladze (new)	46.1	53.1
Ethanol/ chromium$_{polished}$ thin layer on circular copper plate [8]	0.0045	1.47	35.501	−2.02	78–222	4.3–34	27.9–1103	3.2–148	Rohsenow	7.7	23.3
									Pioro	5.5	30.5
									Labuntsov	−27.1	31.1
									Kruzhilin	−28.9	34.4
									Kutateladze (old)	−35.7	37.5
									Kutateladze (new)	24.8	40.3
Ethanol/ St. St.$_{plate}$, $Ra = 0.75$	0.0084	1	48.981	−2.04	20.6–88	5.3–14.1	1.5–45	0.23–5.8	Pioro	3.7	20.2
									Rohsenow	2.9	20.4
									Labuntsov	−36.6	34.4
									Kruzhilin	−32.4	35.4
									Kutateladze (new)	36.4	48.3
									Kutateladze (old)	−50.7	51.7
R-113/copper$_{plate}$ oxidized, $Ra = 1.37$	0.0022	2.25	168.885	−3.14	32–79	10.6–15.7	3.2–24.8	0.24–2.3	Rohsenow	−1.7	12.5
									Pioro	2.1	12.7
									Labuntsov	−8.2	16.3
									Kruzhilin	−13.8	20.3
									Kutateladze (old)	−34	35.2
									Kutateladze (new)	64.9	71.8
R-113/aluminum$_{plate}$ oxidized, $Ra = 3.61$	0.013	1.20	45.62	−2.35	20–71	6.2–14.9	1.6–23.6	0.26–2	Pioro	2	9.4
									Rohsenow	3.1	9.7
									Labuntsov	−28.2	28.9
									Kruzhilin	−31.6	32.4
									Kutateladze (new)	31.1	33.6
									Kutateladze (old)	−48.9	49.1

Table 2 (*continued*)

Fluid–surface	C_{sf}	n	$C^*_{sf} \times 10^{-3}$	m	T_s, °C	ΔT_b, °C	q, kW m^{-2}	h_b, kW m^{-2} K^{-1}	Correlation	Mean error, %	RMS error, %
1	2	3	4	5	6	7	8	9	10	11	12
R-113/brass$_{plate,\ Ra=0.47}$	0.013	1.20	45.62	−2.35	25.6–70	6.2–12.1	1.3–21	0.2–1.8	Rohsenow	−1.8	9.9
									Pioro	−2.7	10
									Kutateladze (new)	24.2	28.1
									Labuntsov	−32.1	32.9
									Kruzhilin	−36.3	37
									Kutateladze (old)	−52	52.3
R-113/St. St.$_{plate,\ Ra=0.47}$	0.013	1.20	45.62	−2.35	31–64	6.9–12.4	3.6–13.8	0.49–1.5	Rohsenow	−4.2	13.6
									Pioro	−5	13.7
									Kutateladze (new)	19.8	25.5
									Labuntsov	−34	35
									Kruzhilin	−37.4	38.3
									Kutateladze (old)	−52.6	53
n-Heptane/ chromium$_{polished\ thin,\ layer\ on\ circular\ copper\ plate}$ [8]	0.014	1.37	13.33	−2	95–185	10–33.7	40–440	2.8–24.7	Rohsenow	0.55	11.3
									Pioro	6.5	13.4
									Labuntsov	−7.3	16.1
									Kutateladze (old)	−12.8	16.2
									Kruzhilin	−18.6	23.1
									Kutateladze (new)	53.3	57.4

Explanations to 2.

Fluids are listed in the following order: water, alcohols, fluorocarbons (refrigerants), and hydrocarbons.

Materials of the surfaces are located according to the value of thermal conductivity: from highest to lowest.

All surfaces are located horizontally.

Two-phase thermosyphon type chambers were used, with the boiling surface (plates) located at the bottom and the condensing part located at the top.

In [9–11] plates (411 × 51 mm) from copper (no surface treatment, naturally oxidized, $\delta = 6.4$ mm, $R_a = 1.37$ (μm), aluminum (surface machined and oxidised, $\delta = 12.7$ mm, $R_a = 3.61$ μm), brass (no surface treatment, $\delta = 6.4$ mm, $R_a = 0.47$ μm), and SS304 stainless steel (no surface treatment, $\delta = 9.62$ mm, $R_a = 0.75$μm) were used.

Working fluid level was 2.4 mm for aluminum plate, 2.4; 3.4; and 5.8 mm for other plates.

In [8], thick copper circular plate ($D = 101.6$ mm, $\delta = 37.8$ mm) with 0.051 mm of polished electroplated chromium was used. Working fluid level was 19.05 mm.

These correlations are listed and described in Table 1. The prediction accuracy of the correlations was assessed and compared. Both correlations of Kutateladze [1,2], and the correlations of Labuntsov [3] and Kruzhilin [4] represent the first approach, as mentioned in the Introduction (i.e., the constants and powers in these correlations do not depend on the type of fluid and the boiling surface characteristics, hence they can be applied to a variety of surface–fluid combinations).

The Rohsenow [5] and Pioro [11] correlations represent the second approach (i.e., the constants in these correlations do depend on the surface–fluid combination, the exponential power in the Prandtl number does depend on the fluid type, and they can be applied mainly to the investigated or tested surface–fluid combinations, as given in [7,11]). The constants in these correlations and the exponential power in the Prandtl number were obtained as the best fit of experimental data for each surface–fluid combination.

All selected nucleate pool-boiling correlations (see Table 1) are well known and widely used in engineering practice.

The results of this comparison are presented in Table 2, and in Figs. 1–6.

The prediction errors were evaluated using the following definitions:

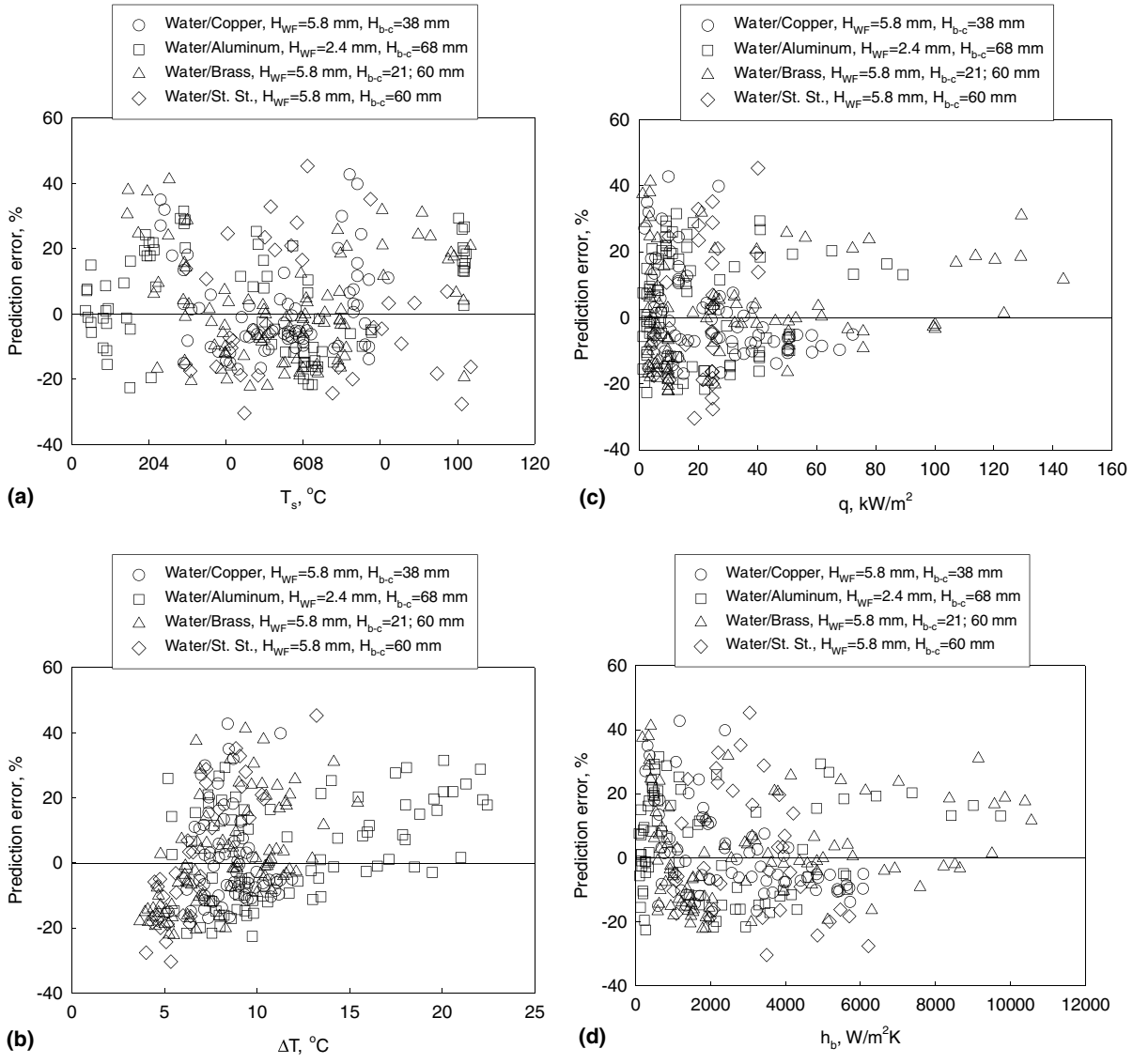

Fig. 1. Accuracy of the Rohsenow correlation.

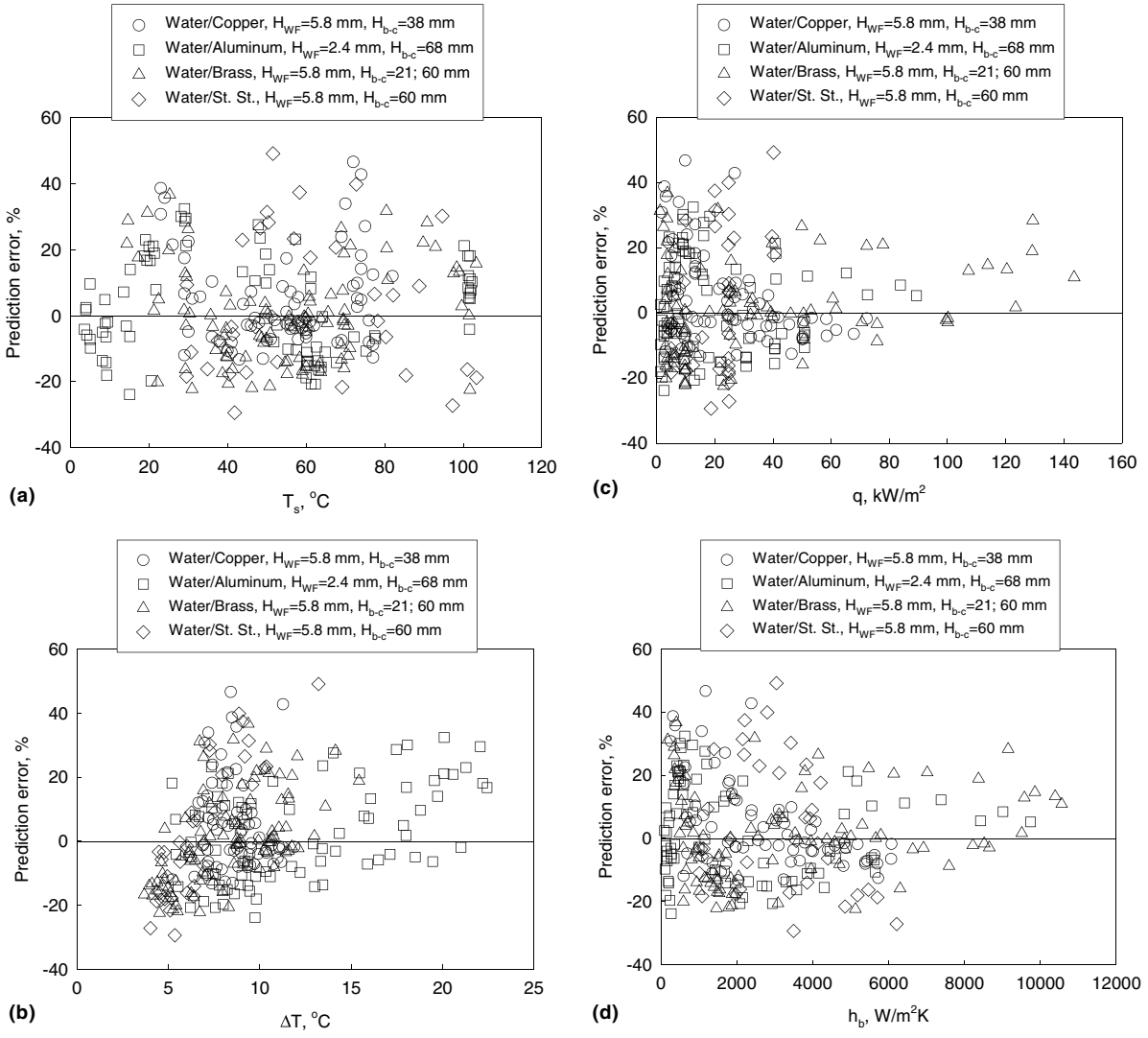

Fig. 2. Accuracy of the Pioro correlation.

$$\text{Error} = \frac{\text{HTC}_{\text{pred}} - \text{HTC}_{\text{exp}}}{\text{HTC}_{\text{exp}}} \tag{7}$$

$$\text{Mean error} = \sum_{i=1}^{n} \frac{\text{Error}_i}{n} \tag{8}$$

$$\text{RMS error} = \sqrt{\sum_{i=1}^{n} \frac{\text{Error}_i^2}{n}} \tag{9}$$

Figs. 1–6 show the prediction errors between the experimental data and the corresponding results predicted by the following correlations: Rohsenow (Fig. 1), Pioro (Fig. 2), Kutateladze "new" (Fig. 3) and "old" (Fig. 4), Labuntsov (Fig. 5), and Kruzhilin (Fig. 6). The experimental data refer to those data obtained during nucleate pool boiling of water on thick large-size horizontal plates made from copper, aluminum, brass, and stainless steel.

These figures show the *prediction error versus*: (i) *saturation temperature* (Figs. 1(a)–6(a)), (ii) *temperature difference* (Figs. 1(b)–6(b)), (iii) *heat flux* (Figs. 1(c)–6(c)), and (iv) *HTC* (Figs. 1(d)–6(d)). It is clearly seen that only the correlations of Rohsenow and Pioro have lower values of prediction errors (from −20% to +40%) within the investigated range of saturation temperature, heat flux, temperature difference, and HTC. In general, the prediction errors for the remaining correlations increase with decreasing saturation temperature, heat flux, and

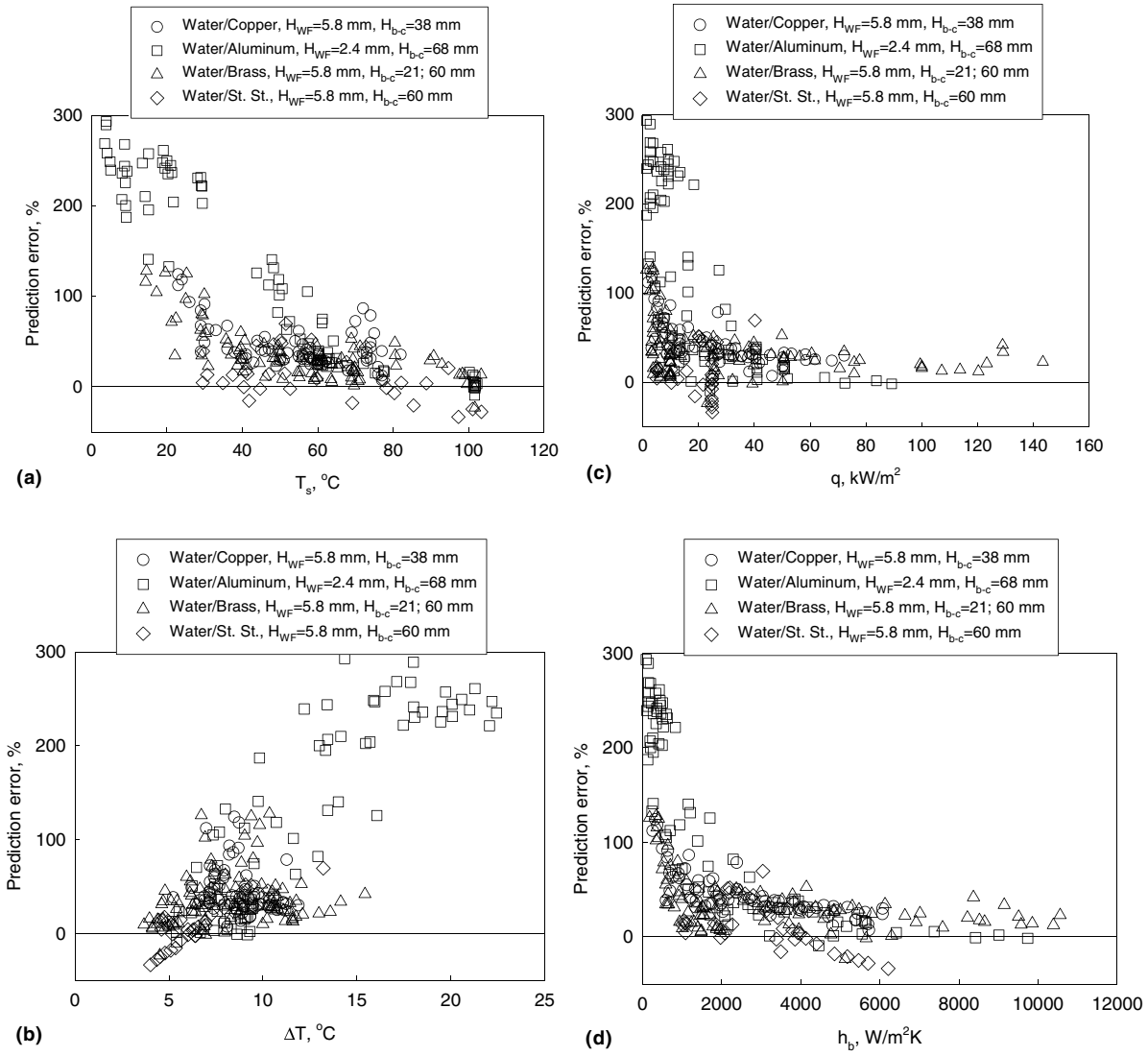

Fig. 3. Accuracy of the Kutateladze "new" correlation.

HTC values. The maximum prediction error can be as high as 300% for the Kutateladze "new" correlation, about −60% to +40% for the Kutateladze "old" correlation, and up to 140% for the Labuntsov and Kruzhilin correlations.

3. Conclusions and final remarks

The analysis shows that within the investigated range of boiling conditions, working fluids, and boiling surfaces, the following ranking of the tested correlations can be made:

The Rohsenow and Pioro correlations (i.e., those applying the second approach, with the constants and powers for the Prandtl number depending on a surface–fluid combination obtained from the experimental data) are the more accurate than the other correlations, which apply the first approach.

As indicated in Part I of this paper, the effect of surface characteristics on the boiling process depends on thermophysical properties of the surface (thermal conductivity and thermal absorption), interaction between the solid surface, liquid and vapor, surface microgeometry (dimensions and shape of cracks and pores), etc. All these parameters affect the HTC simultaneously

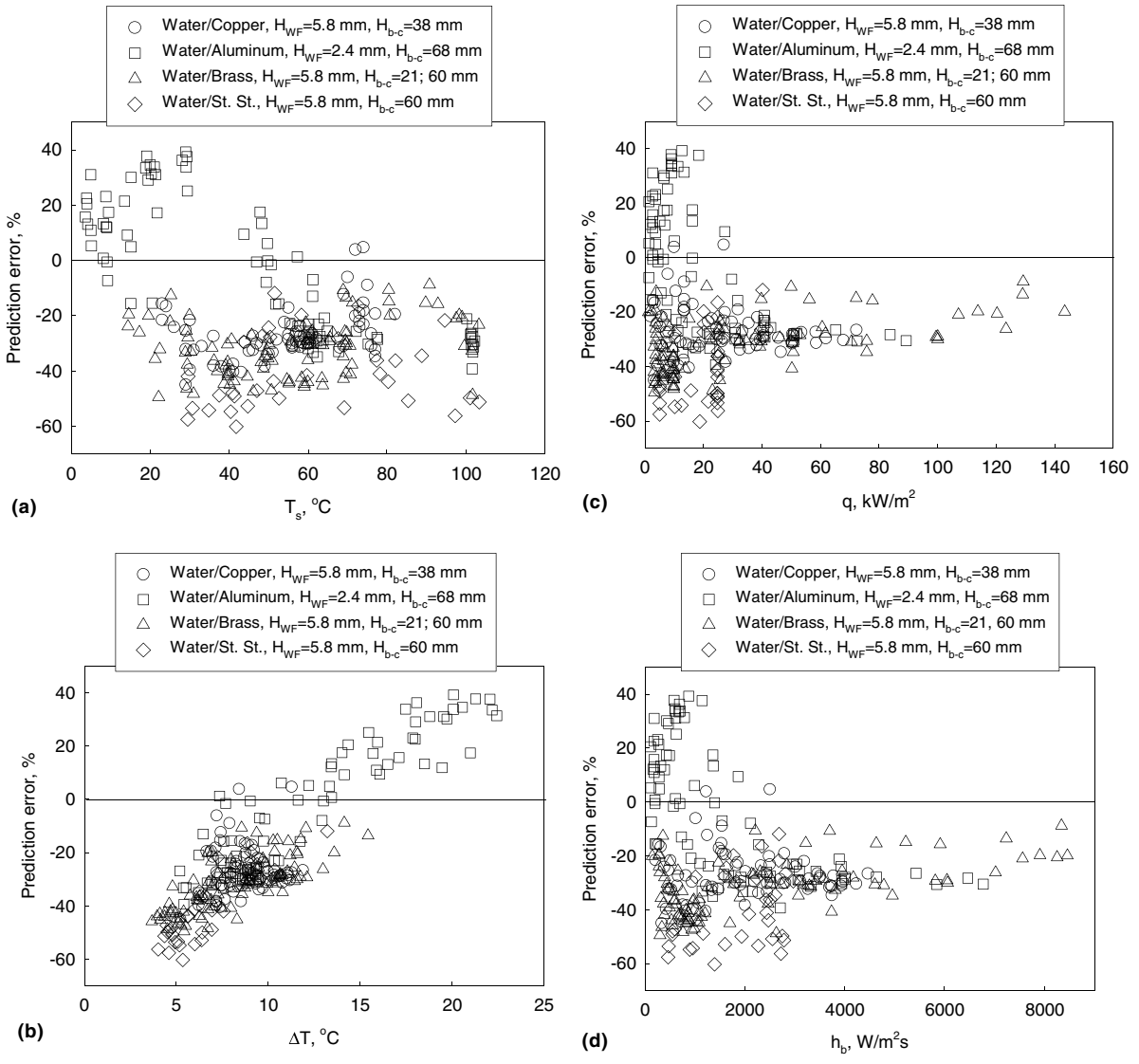

Fig. 4. Accuracy of the Kutateladze "old" correlation.

and are interlinked. However, there are still not enough data available to solve this complex problem. Due to these complexities, the available correlations do not take into account all the specified parameters, thus lowering prediction accuracy.

Appendix 1. Surface-roughness parameters

A laser profilometer was used to determine the surface-roughness parameters that are listed in Table A1.1. The characteristics of the laser profilometer itself were as follows: Vertical measuring range—±300 μm; scanning speed—80 mm min^{-1}; number of measured points—2000; wavelength cut-off (L_c)—1.0 mm; stylus filter (N_f)—50 μm; and scan length—10 mm.

Explanation to Table A1.1

Simple-roughness-amplitude parameters:

Mean parameters

R_a—average roughness: area between the roughness profile and its mean line or its integral of the absolute value of the roughness-profile height over the evaluation length. The average roughness is the most commonly used parameter in surface-finish measurements.

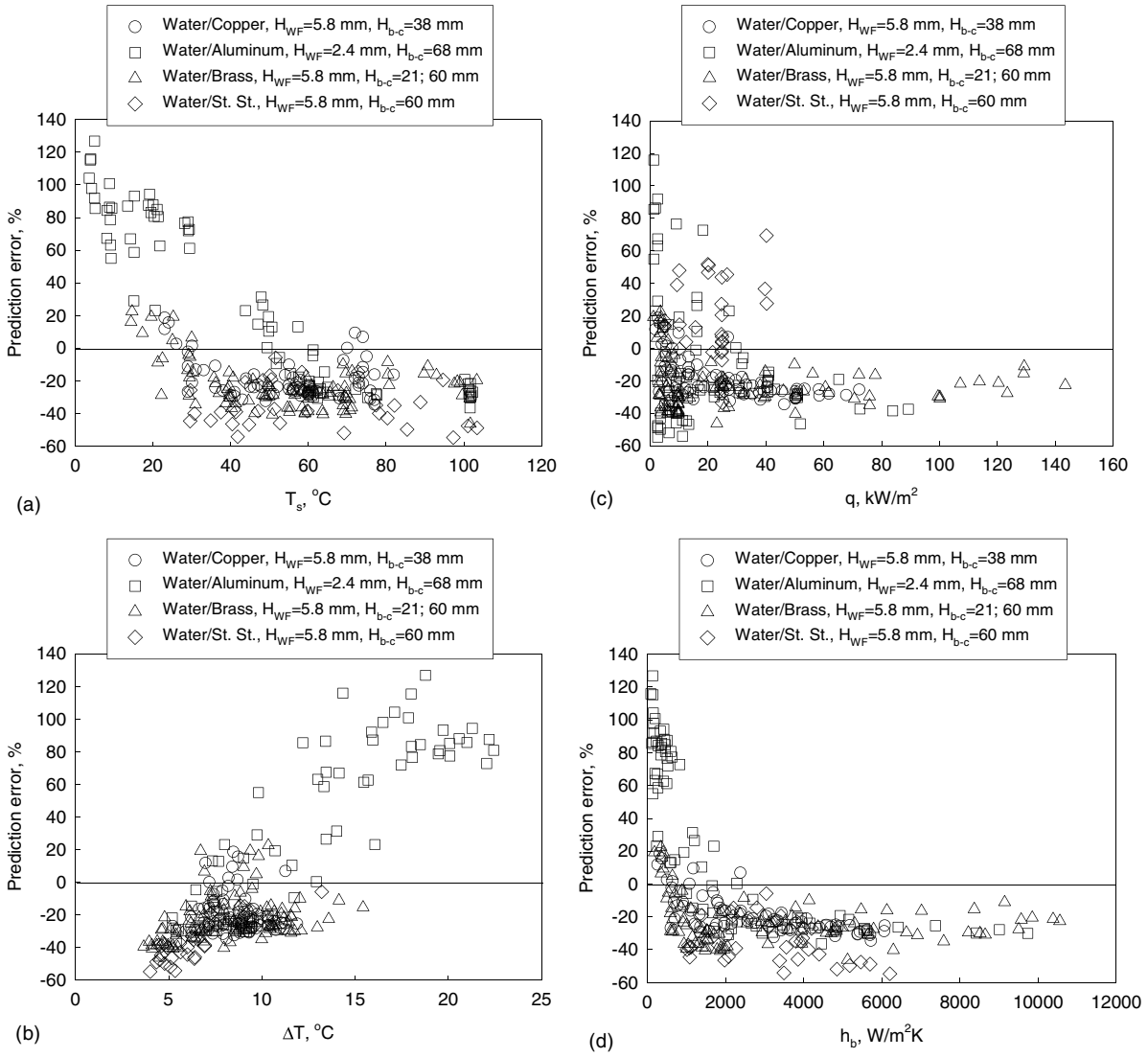

Fig. 5. Accuracy of the Labuntsov correlation.

R_q—root-mean-square roughness (rms roughness): average roughness parameter calculated as a square root from another integral of the surface-roughness profile. Root-mean-square roughness was a commonly used parameter in the past; however, nowadays it has been replaced with R_a in metal-machining specifications. Usually (but not necessarily), R_q is 1.1–1.3 times larger than R_a.

Extreme parameters

R_p—peak roughness (height of the highest peak in the roughness profile over the evaluation length).

R_v—depth roughness (depth of the deepest valley in the roughness profile over the evaluation length).

R_t—total roughness (vertical distance from the deepest valley to the highest peak), $R_t = R_p + R_v$.

Mean-extreme parameters

R_{pm}—mean-peak roughness (average peak roughness over the sample length).

R_z—mean-total roughness (average value of the five highest peaks plus the five deepest valleys over the evaluation length).

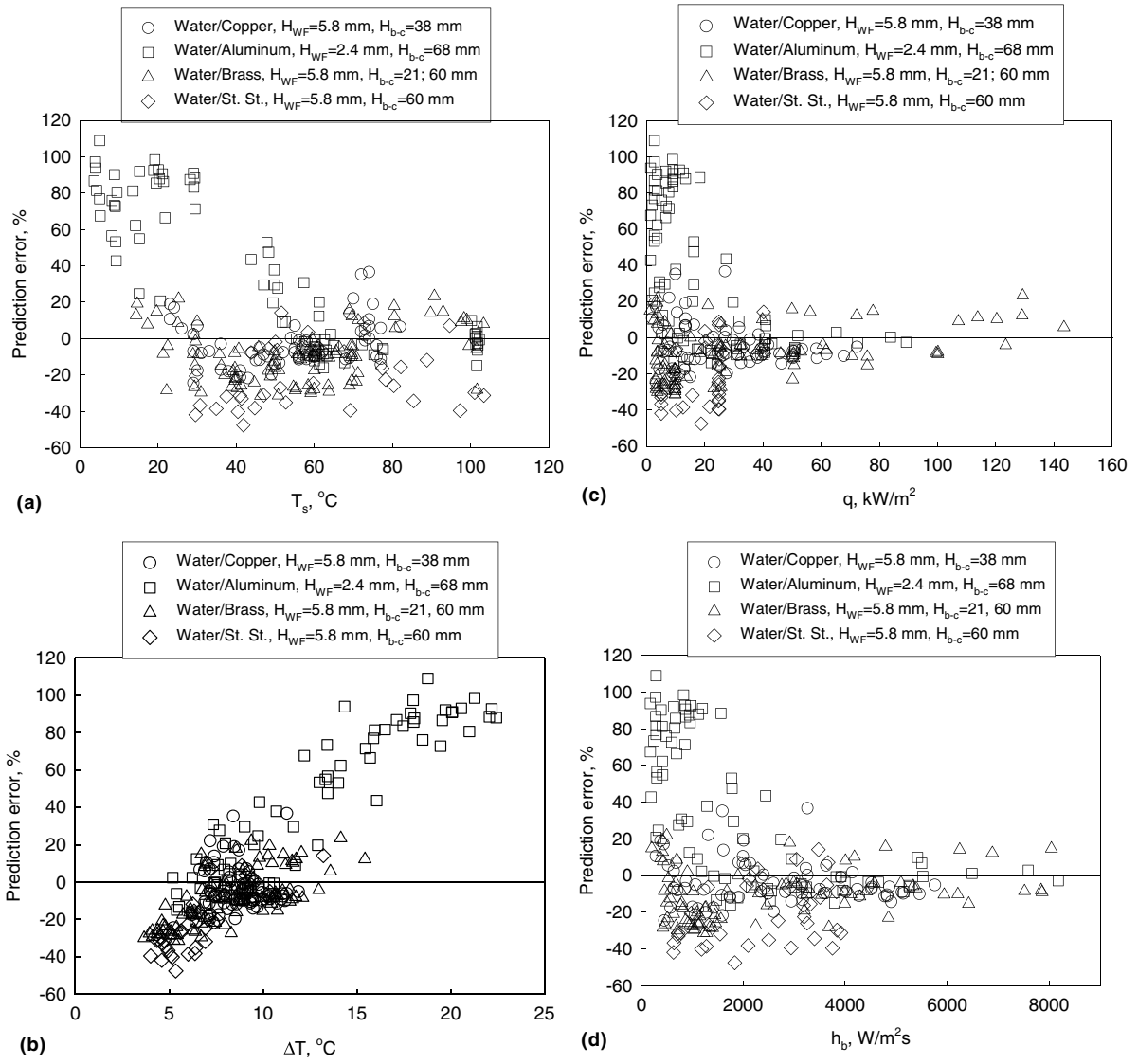

Fig. 6. Accuracy of the Kruzhilin correlation.

R_{z3}—mean-total roughness of third extremes parameters (average vertical distance from the third deepest valley to the third highest peak).

Mean-extreme parameters are less sensitive to single unusual features, such as artificial scratches, gouges, burrs, etc.

Roughness-spacing parameters

HPC—high-peak count per length (number of peaks per length that cross above a certain threshold and then go back below it).

Mean-roughness-spacing parameters

S_m—mean spacing between peaks (peaks cross above a mean line and then go back below it).
λ_a—average wavelength of surface.
λ_q—rms average wavelength of surface.

Roughness-hybrid parameters

Δ_a—average of absolute slope of roughness profile over the evaluation length.
L_o—actual profile length (in all measurements, this was 8 mm).

Table A1.1
Average surface roughness parameters of large-size plates

Plate material	R_a (μm)	R_q (μm)	R_p (μm)	R_v (μm)	R_t (μm)	R_{pm} (μm)	R_z (μm)	R_{3z} (μm)	HSC (–)	S_m (μm)	λ_a (μm)	λ_q (μm)	Δ_a (degr)	R_{sk} (μm)
Copper	1.4	1.7	7.2	4.4	12	5.2	9	6.4	68	117	109	107	0.08	0.38
Al	3.6	4.5	14	14	28	12	22	17	89	89	88	82.9	0.26	0.47
Brass	0.5	0.7	2.4	5.1	7.4	1.7	3.9	2.4	126	63	65	70.1	0.05	−1.28
St. St.	0.5	0.6	3.4	2.5	5.9	2.1	3.8	2.5	123	64	65	65.2	0.05	0.19
Minimum and maximum values of the roughness parameters														
Min.	0.5	0.6	2.4	2.5	5.9	1.7	3.8	2.4	68	63	65	65.2	0.05	−1.28
Max.	1.4	4.5	14	14	28	12	22	17	126	117	109	107	0.26	0.47

Statistical parameters:

R_{sk}—skewness (this parameter represents the profile variation symmetry over its mean line). Surfaces with $R_{sk} < 0$ have fairly deep valleys in a smoother plateau. Surfaces with $R_{sk} > 0$ have fairly high spikes, which protrude above a flatter average.

References

[1] S.S. Kutateladze, V.M. Borishanskii, A Concise Encyclopedia of Heat Transfer, Pergamon Press, New York, NY, USA, 1966 (Chapter 12).

[2] S.S. Kutateladze, Heat Transfer and Hydrodynamic Resistance: Handbook, Energoatomizdat Publishing House, Moscow, Russia, 1990, Chapter 12.7 (in Russian).

[3] D.A. Labuntsov, Heat transfer problems with nucleate boiling of liquids, Thermal Engineering 19 (9) (1972) 21–28.

[4] G.N. Kruzhilin, Free-convection transfer of heat from a horizontal plate and boiling liquid, Doklady AN SSSR (Reports of the USSR Academy of Sciences) 58 (8) (1947) 1657–1660 (in Russian).

[5] W.M. Rohsenow, A method of correlating heat transfer data for surface boiling of liquids, Transactions of the ASME 74 (1952) 969–976.

[6] W.M. Rohsenow, J.P. Hartnett, Y.I. Cho (Eds.), Handbook of Heat Transfer, 3rd edition, McGraw-Hill, New York, NY, USA, 1998, pp. 15.46–15.47.

[7] I.L. Pioro, Experimental evaluation of constants for the Rohsenow pool boiling correlation, International Journal of Heat and Mass Transfer 42 (1999) 2003–2013.

[8] M. Cichelly, C. Bonilla, Heat transfer to liquids boiling under pressure, Transactions of AIChE 41 (1945) 755–787.

[9] Y. Lee, I. Pioro, H.J. Park, An experimental study on a plate type two-phase closed thermosyphon, in: Proceedings of the 4th International Heat Pipe Symposium, Tsukuba, Japan, May 1994, pp. 49–58.

[10] I.L. Pioro, H.J. Park, Y. Lee, Heat transfer in a two-phase closed thermosyphon: horizontally flat plate type, in: Proceedings of the 5th International Symposium on Thermal Engineering and Science for Cold Regions, Ottawa, ON, Canada, May 1996, pp. 489–494.

[11] I. Pioro, Boiling heat transfer characteristics of thin liquid layers in a horizontally flat two-phase thermosyphon, Preprints of the 10th International Heat Pipe Conference, Stuttgart, Germany, September 1997, Paper H1-5.